Copper – Lead – Antimony

Kostyantyn Korniyenko

Introduction

Scientific interest in the phase equilibria in the Cu-Pb-Sb system is due, in particular, to the effect of the third component on the properties of lead-antimony binary alloys, especially of lead rich alloys in which dispersion hardening was found [1928Mor]. Copper as the third component forms several compounds with antimony as well as solid solutions, but with lead it forms a liquid miscibility gap and no appreciable solid solution. Owing to the compound formation, copper increases the apparent solubility of antimony. The excess antimony is tied up with the copper and so is not available for dispersion hardening. The constitution of Cu-Pb-Sb alloys was investigated first by [1899Cha]. Subsequently, the liquidus surface [1923Sch, 1928Mor, 1941Sch, 1963Dav, 1966Kry], reaction scheme, phase equilibria at subsolidus temperatures, Sb-Cu76.5Pb23.5 vertical section [1941Sch] and isothermal section at 1200°C [1990Esp] have been studied. The existence of a miscibility gap in the system was established. [1941Hof, 1954Sch] investigated crystal structures of the constituents of the Cu-Pb-Sb alloys. [1972Dee, 1963Dav, 1973Kir, 1974Kir, 1991Esp1, 1991Esp2] studied thermodynamic properties. [1975Heu] studied the process of grain refinement of hypoeutectic Pb-Sb alloys through the addition of Cu and reported the corresponding phase relations. The experimental details of studies of phase equilibria are presented in Table 1. However, information relating to the phase equilibria in the Cu-Pb-Sb system is incomplete, in particular, with respect to the reaction scheme. Through further study of the system, the possibilities of practical applications of copper-lead-antimony alloys will be extended.

Binary Systems

The Cu-Pb and Cu-Sb binary systems are accepted from the MSIT Evaluation Program [2006Sch] and [2006Rok], respectively. The Pb-Sb system is accepted from [Mas2].

Solid Phases

No ternary phases have been reported. Crystallographic data concerning the known unary and binary phases are listed in Table 2. [1928Mor] studied the effect of Cu on the solid solubility of Sb in (Pb), and found that the presence of small amounts of copper has a tendency to increase the solubility, at least at higher temperatures (Table 2).

Invariant Equilibria

Table 3 lists temperatures, types of reactions and the compositions of the phases taking place in the invariant equilibria that have been established unambiguously. Phase compositions from [1941Sch] have been recalculated from mass to atomic percent. The reaction scheme, with corrections to maintain consistency with the binary systems, is shown in Fig. 1.

Liquidus Surface

The liquidus surface projection of the system is shown in Figs. 2a, 2b. It is based mainly on the experimental investigations of [1941Sch]. Constitution in the Pb rich corner was also determined by [1963Dav] and [1966Kry]. From Fig. 2, it can be seen that the miscibility gap in the ternary system is wider than in the Cu-Pb binary and extends to lower temperatures - from 980.5°C in the binary system to 619°C at the critical point of the ternary. The location of the critical point (c_1) is 35.22Cu-35.58Pb-29.2Sb (at.%) [1941Sch].

Isothermal Sections

The isothermal section at 1200°C (Fig. 3) has been constructed by [1990Esp] showing a liquid miscibility gap. The rest of the section is completely liquid.

Temperature – Composition Sections

The Sb-$Cu_{76.5}Pb_{23.5}$ vertical section is shown in Fig. 4 after [1941Sch] with corrections to maintain consistency with the accepted Cu-Pb binary system.

Thermodynamics

Thermodynamic properties of liquid metallic copper-lead-antimony solutions have been investigated for the first time by [1963Dav] in the Pb rich corner, and by [1972Dee] using emf measurements in the range 1100-1200°C. The activity, the activity coefficients of the components and the integral values of the excess thermodynamic functions for the liquid phase in the ternary system have been calculated. The liquid ternary alloys exhibit positive-negative deviations from ideality. Thermodynamic analysis of the behavior of the intermetallides in the ternary system over the temperature interval 627 to 1027°C was carried out by [1973Kir] using their own experimental measurements and those obtained by other authors. The same authors in [1974Kir] have presented the excess Gibbs energy of liquid alloys at 1027°C. The excess entropy was calculated from the temperature dependence of the Gibbs energy. The method used by [1974Kir] for the Gibbs energy measurement was not indicated in their work. It should be mentioned that the data of [1972Dee] and [1973Kir] are in a poor agreement with each other and neither indicate decomposition of the liquid in the ternary system. Activities of the component elements were determined at 1200°C by [1991Esp1] and [1991Esp2] using the transportation method, based on vapor pressure measurement of Pb and Sb. Isoactivity curves of antimony and lead determined in [1991Esp2] are shown in Figs. 5 and 6, respectively. Isoactivity curves of copper were calculated in [1991Esp2] based on data for Sb and Pb activity. They are shown in Fig. 7. The activity results of Cu, Pb and Sb determined at 1150 °C by [1972Dee] do not show any kinks in the miscibility gap and thus they are not consistent with the results of [1991Esp2]. In the single phase fields, the agreement between these two investigations is also poor. The data of [1991Esp2] are preferred in the present work because they are consistent with the phase diagram demonstrating kinks in the activity curves in the region of the miscibility gap. One can see that in the two-phase L' + L" region Sb activity is below 0.1, exhibiting a large negative deviation from Raoult's law, while the activity of Pb ranges from 0.75 to 0.95. A high activity of lead is maintained due to the dissolution of copper in the lead rich liquid which exhibits a tendency for immiscibility in the Cu-Pb binary system.

Notes on Materials Properties and Applications

Lead-antimony castings are used in the electric industry, especially for the production of battery grids [1975Heu]. Hot tearing can be avoided by suitable grain refinement. Small copper additions to a $Pb_{95.82}Sb_{4.18}$ alloy supplies the high grain refining effect. Increasing the copper content above 0.13 at.% does not further improve the grain refinement. Compression tests of the alloys having a lead content greater than 41.7 at.% were carried out by [1899Cha]. The maximum load corresponding to compressions of 0.2 and 7.5 mm was found for the $Cu_{29.3}Pb_{46.4}Sb_{24.3}$ and $Cu_{29.3}Pb_{46.4}Sb_{24.3}$ alloys, respectively. The effect of copper (0.22 at.%) on the tensile strength of Pb-Sb alloys (0 to 9.78 at.% Sb) was studied by [1928Mor]. It was concluded that small amounts of copper have the effect of shifting the dispersion hardness peak of Pb-Sb alloys toward higher antimony contents.

Miscellaneous

The kinetics of nucleation were studied by [1966Kry]. An attempt to explain decoppering in the copper trap was undertaken through microscopic observation.

References

[1899Cha] Charpy, G., "Alloys of Lead, Copper and Antimony", *Metallographist*, **2**, 44-46 (1899) (Morphology, Experimental, Mechan. Prop., 0)

[1923Sch] Schack, H., "The Ternary System Copper-Lead-Antimony" (in German), *Z. Anorg. Chem.*, **132**, 265-272 (1923) (Morphology, Phase Diagram, Experimental, 4)

[1928Mor] Morgen, R.A., Swenson, L.G., Nix, F.C., Roberts, E.H., "The System Lead-Antimony-Copper", *Trans. Amer. Inst. Min. Met Eng.*, 317-327 (1928) (Morphology, Phase Diagram, Phase Relations, Experimental, Mechan. Prop., 14)

[1941Hof] Hofmann, W., "X-ray Diffraction Analysis Study of the Antimony-Copper and Antimony-Lead-Copper Alloys" (in German), *Z. Metallkd.*, **33**(2), 61-62 (1941) (Crys. Structure, Experimental, 1)

[1941Sch] Schrader, A., Hanemann, H., "On the System Lead-Antimony-Copper" (in German), *Z. Metallkd.*, **33**(2), 49-60 (1941) (Phase Diagram, Experimental, #, 36)

[1954Sch] Schubert, K., Ilschner, M., "Investigations in the System Copper-Antimony" (in German), *Z. Metallkd.*, **45**(6), 366-370 (1954) (Crys. Structure, Phase Diagram, Experimental, 20)

[1958Gue] Günzel, E., Schubert, K, "Structural Investigations in the System Copper-Antimony", *Z. Metallkd.*, **49**, 124-133 (1958) (Crys. Structure, Phase Diagram, Experimental, 21)

[1963Dav] Davey, T.R.A., "Phase Systems Concerned with the Copper Drossing of Lead", *Bull. Inst. Min. Met.*, **72**, 553-620 (1963) (Phase Diagram, Thermodyn., Experimental, Review, Theory)

[1964Pea] Pearson, W.B., "Electrical Resistivity, Hall Coefficient and Thermoelectric Power of $AuSb_2$ and Cu_2Sb", *Canad. J. Phys.*, **42**, 519-525 (1964) (Crys. Structure, Experimental, Electr. Prop.)

[1966Kry] Krysko, W.W., "The Decoppering of Pb: The Parts 5-7" (in German), *Z. Erzberg. Metallhuettenwesen*, **19**(3), 121-127 (1966) (Morphology, Phase Relations, Experimental, Kinetics, 17)

[1972Dee] Deev, V. I., Goldobin, V. P., Rybnikov, V. I., Smirnov, V. I., "Thermodynamic Properties of Liquid Ternary Copper-Lead-Antimony Alloys", *J. Phys. Chem.*, **46**(6), 811-814 (1972) (Thermodyn., Experimental, Calculation, 8)

[1973Kir] Kirov, A.S., Boychev, A.P., Neykova, E.A., Denev, D.G., "Thermodynamics of the Intermetallides in the System of Lead-Copper-Antimony", *Dokl. Bolg. Akad. Nauk*, **26**(11), 1505-1508 (1973) (Thermodyn., Experimental, 5)

[1974Kir] Kirov, A.S., Boychev, A.P., Neykova, E.A., Denev, D.G., "Thermodynamic Properties of Alloys from the Ternary System of Lead-Copper-Antimony", *Dokl. Bolg. Akad. Nauk*, **27**(2), 231-233 (1974) (Thermodyn., Experimental, 5)

[1975Heu] Heubner, U., Mueller, I., Ueberschaer, A., "Grain Refinement of Hypoeutectic Lead-Antimony Alloys by Additions of Copper and Sulfur", *Z. Metallkd.*, **66**(2), 74-79 (1975) (Morphology, Phase Relations, Experimental, 18)

[1990Esp] Espeleta, A.K., Hino, M., Azakami, T., "Phase Separation and Silver and Gold Distribution in the Pb-Fe-Sb and Pb-Cu-Sb Systems at 1200°C", *Shigen to Sozai*, **106**(13), 53-58 (1990) (Phase Diagram, Phase Relations, Experimental, #, 11)

[1991Esp1] Espeleta, A.K., Hino, M., Azakami, T., "Activity Determination in the Pb-Fe-Sb and Pb-Cu-Sb Ternary Systems by the Transportation Method", *Shigen to Sozai*, **107**(1), 53-59 (1990) (Thermodyn., Experimental, 10)

[1991Esp2] Espeleta, A.K., Hino, M., Azakami, T., "Activity of Component Elements in the Pb-Fe-Sb and Pb-Cu-Sb Ternary Systems", *Met. Rev. MMIJ*, **8**(1), 80-97 (1991) (Phase Relations, Thermodyn., Experimental, 10)

[1991Tep] Teppo, O., Niemelae, J., Taskinen, P., "The Copper-Lead Phase Diagram", *Thermochim. Acta,* **185**(1), 155-169 (1991) (Phase Diagram, Thermodyn., Review, #, 17)

[2006Rok] Rokhlin, L., Bochvar, N., "Cu-Sb (Copper-Antimony)", MSIT Binary Evaluation Program, in *MSIT Workplace*, Effenberg, G. (Ed.), MSI, Materials Science International Services GmbH, Stuttgart; to be published, (2006) (Crys. Structure, Phase Diagram, Assessment, #, *, 19)

[2006Sch] Schmid-Fetzer, R., Shcherban, O., Tomashik, V., Jialin, Y., "Cu-Pb (Copper-Lead)", MSIT Binary Evaluation Program, in *MSIT Workplace*, Effenberg, G. (Ed.), MSI, Materials Science International Services GmbH, Stuttgart, to be published (2006) (Crys. Structure, Phase Diagram, Assessment, #, 7)

Table 1: Investigations of the Cu-Pb-Sb Phase Relations, Structures and Thermodynamics

Reference	Method/Experimental Technique	Temperature/Composition/Phase Range Studied
[1899Cha]	Optical microscopy	41.7 to 100 at.% Pb
[1923Sch]	Optical microscopy, thermal analysis (cooling curves)	327 - 1084°C, whole range of compositions
[1928Mor]	Optical microscopy, thermal analysis (cooling curves), chemical analysis	327 - 1084°C, whole range of compositions
[1941Hof]	X-ray Debye-Scherrer studies	Cu alloys with 15.5, 19, 25.4 at.% Sb and Pb additions
[1941Sch]	Thermal analysis, X-ray studies	< 1084°C, whole range of compositions
[1963Dav]	Solubilities of the precipitating phases determination	327 - 600°C, the Pb rich corner
[1966Kry]	Optical microscopy, chemical analysis	300 - 900°C, the Pb rich corner
[1972Dee]	Emf measurements	1100 - 1200°C, whole range of compositions
[1973Kir]	Copper antimonides stabilities determination	627 - 1027°C
[1974Kir]	Excess isobaric-isothermal potential and excess entropy determination	627 - 1027°C; mole fraction ratios - Cu:Sb = 3:1; Pb:Cu = 1:9, 1:1, 9:1
[1975Heu]	Optical microscopy, grain refinement	500°C, the Pb based alloys with 4.2 at.% Sb and ≤ 0.13 at.% Cu
[1990Esp]	EMPA	1200°C, ≤ 30 at.% Sb
[1991Esp1]	Transportation method	1200°C, whole range of compositions
[1991Esp2]	Transportation method	1200°C, whole range of compositions

Table 2: Crystallographic Data of Solid Phases

Phase/ Temperature Range [°C]	Pearson Symbol/ Space Group/ Prototype	Lattice Parameters [pm]	Comments/References
(Cu) < 1084.62 $Cu_{1-x-y}Pb_xSb_y$	*cF*4 $Fm\bar{3}m$ Cu	a = 361.46	at 25°C [Mas2] dissolves 5.8 at.% Sb at 645°C [Mas2] and 0.4 at.% Pb at 952.7°C [2006Sch] $x = 0$, $0 \le y \le 0.004$ at 400°C [Mas2] $y = 0$, $0 \le x \le 0.000046$ at 326.5°C [1991Tep]
(Pb) < 327.502 $Cu_xPb_{1-x-y}Sb_y$	*cF*4 $Fm\bar{3}m$ Cu	a = 495.02	at 25°C [Mas2] dissolves 5.8 at.% Sb at 251.7°C and 0.02 at.% Cu at 326.5°C [2006Sch] at $x = 0$, $0 \le y \le 0.0344$, 238°C [1928Mor] at $x = 0$, $0 \le y \le 0.0213$, 200°C [1928Mor] at $x = 0$, $0 \le y \le 0.003$, 100°C [Mas2] at $y = 0$, $0 \le x < 0.0002$, 326.5°C [1991Tep] at $x = 0.0006$, $0 \le y \le 0.0456$, 238°C [1928Mor] at $x = 0.0006$, $0 \le y \le 0.0285$, 200°C [1928Mor]
(Pb)(I)	*hP*2 $P6_3/mmc$ Mg	a = 326.5 c = 538.7	at 25°C, 10.3 GPa [Mas2]
(Sb) < 630.755 $Cu_xPb_ySb_{1-x-y}$	*hR*6 $R\bar{3}m$ αAs	a = 430.84 c = 1127.4	at 25°C [V-C2] at $x = 0$, $0 \le y \le 0.015$ to 0.027, 252°C [H] at $x = 0$, $0 \le y \le 0.019$, 251.7°C [Mas2]
(Sb)(II)	*cP*1 $Pm\bar{3}m$ αPo	a = 299.2	at 25°C, 5.0 GPa [Mas2]
(Sb)(III)	*hP*2 $P6_3/mmc$ Mg	a = 337.6 c = 534.1	at 25°C, 7.5 GPa [Mas2]
(Sb)(IV)	*mP*3	a = 556 b = 404 c = 422 β = 86.0°	at 25°C, 14.0 GPa [Mas2]

Phase/ Temperature Range [°C]	Pearson Symbol/ Space Group/ Prototype	Lattice Parameters [pm]	Comments/References
γ, $Cu_{1-x-y}Pb_xSb_y$	*hP*2		$x = 0$, $0.155 \leq y \leq 0.16$ [Mas2]
488 - 400	$P6_3/mmc$	$a = 268.8$	$x = 0$, $y = 0.155$, 470°C [1941Hof]
	Mg	$c = 433.3$	
$Cu_{11}Sb_2$		$a = 271$	$x = 0$, $y = 0.155$, 460°C [1954Sch]
488 - 400		$c = 436$	
δ, Cu_4Sb	*hP**		0 at.% Pb, 18.5 to 20 at.% Sb [Mas2]
< 462	$P6_3/mmc$	$a = 272.1$	at 19.0 at.% Sb, annealed at 350°C for
	Cu_4Sb	$c = 431.9$	48 to 88 h [1954Sch]
ζ, $Cu_{10}Sb_3$	*hP*26		0 at.% Pb, 21.3 to 21.6 at.% Sb [Mas2]
~ (390 - 260)	$P\bar{3}$	$a = 992.0$	at 21.5 at.% Sb [1958Gue]
	$Cu_{10}Sb_3$	$c = 431.9$	
ε, Cu_3Sb	*oP*8		0 at.% Pb, 22.8 to 25.3 at.% Sb [Mas2]
~ 445 - 260	*Pmmn*	$a = 550$	[E]
	βTiCu_3	$b = 476$	
		$c = 435$	
		$a = 558.2$	at 24.9 at.%·Sb, 400°C [1954Sch]
		$b = 479.4$	
		$c = 438.7$	
β, $Cu_{1-x-y}Pb_xSb_y$	*oF*16		$x = 0$, $0.194 \leq y \leq 0.308$ [Mas2]
	$Fm\bar{3}m$		
$Cu_{11}Sb_2$	BiF_3	$a = 601$	at $x = 0$, $y = 0.25$, 475°C [H]
683 - ~440			
η, Cu_2Sb	*tP*6		0 at.% Pb, 32 to 33.3 at.% Sb [Mas2]
< 586	*P*4/*nmm*	$a = 400.0$	[H]
	Cu_2Sb	$c = 610.3$	
		$a = 400.12$	at 33 at.% Sb annealed between 550 and
		$c = 610.39$	560°C [1964Pea]

Table 3: Invariant Equilibria

Reaction	T [°C]	Type	Phase	Composition (at.%)		
				Cu	Pb	Sb
L' ⇌ L" + β	640	e_3	L'	5.81	77.51	16.68
			L"	67.02	5.93	27.04
			β	81.37	~ 0.00	18.63
L' ⇌ (Cu) + β + L"	623	E_1	L'	80.04	2.23	17.72
			(Cu)	~ 93.91	~ 0.00	~ 6.09
			β	81.37	~ 0.00	18.63
			L"	3.17	95.18	1.65
L', L", β	619	c_1 (crit. point)	L', L"	35.22	35.58	29.20
			β	81.37	~ 0.00	18.63
β + (Cu) + L ⇌ γ	~ 437	P_1	β	78.81	~ 0	21.19
			(Cu)	94.92	~ 0	5.08
			γ	84.5	~ 0	15.5
			L	0.97	97.86	1.17
L + β ⇌ η + γ	~ 432	U_1	L	2.03	91.44	6.53
L + (Cu) ⇌ γ + (Pb)	324	U_2	L	0.42	99.19	0.39
			(Cu)	97.76	~ 0	2.24
			γ	~ 81.72	~ 0.004	~ 18.27
			(Pb)	~ 0	~ 100	~ 0
L + γ ⇌ η + (Pb)	~ 300	U_3	L	1.43	95.16	3.40
			γ	~ 76.93	~ 0.004	~ 23.07
			η	~ 66.67	~ 0.004	~ 33.33
			(Pb)	0.03	99.80	0.17
L ⇌ (Pb) + η + (Sb)	248.6	E_2	L	0.18	79.57	20.25
			(Pb)	~ 0	~ 96.98	~ 3.02
			η	~ 66.67	~ 0	~ 33.33
			(Sb)	~ 0	~ 1.9	~ 98.1

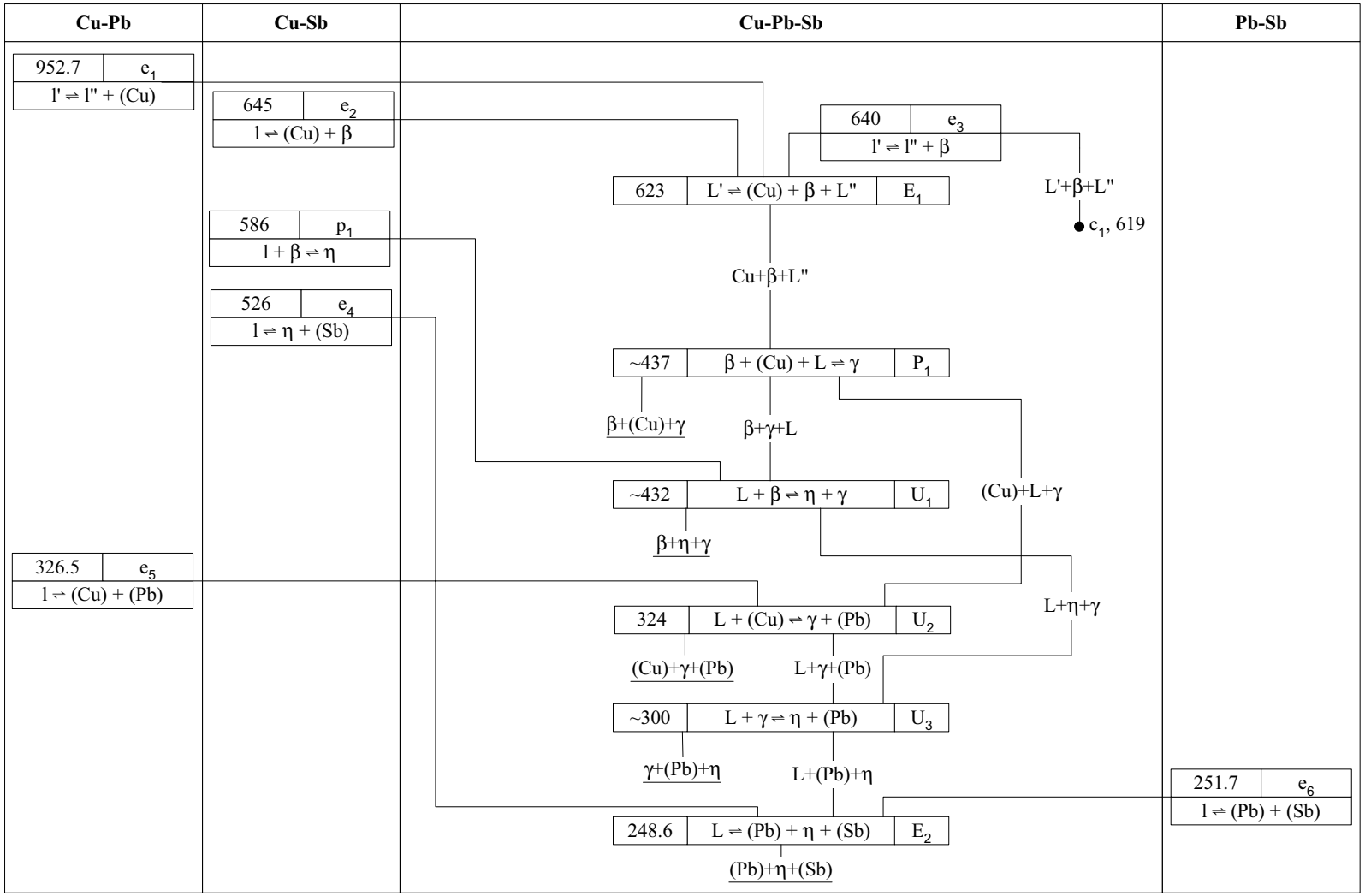

Fig. 1: Cu-Pb-Sb. Reaction scheme

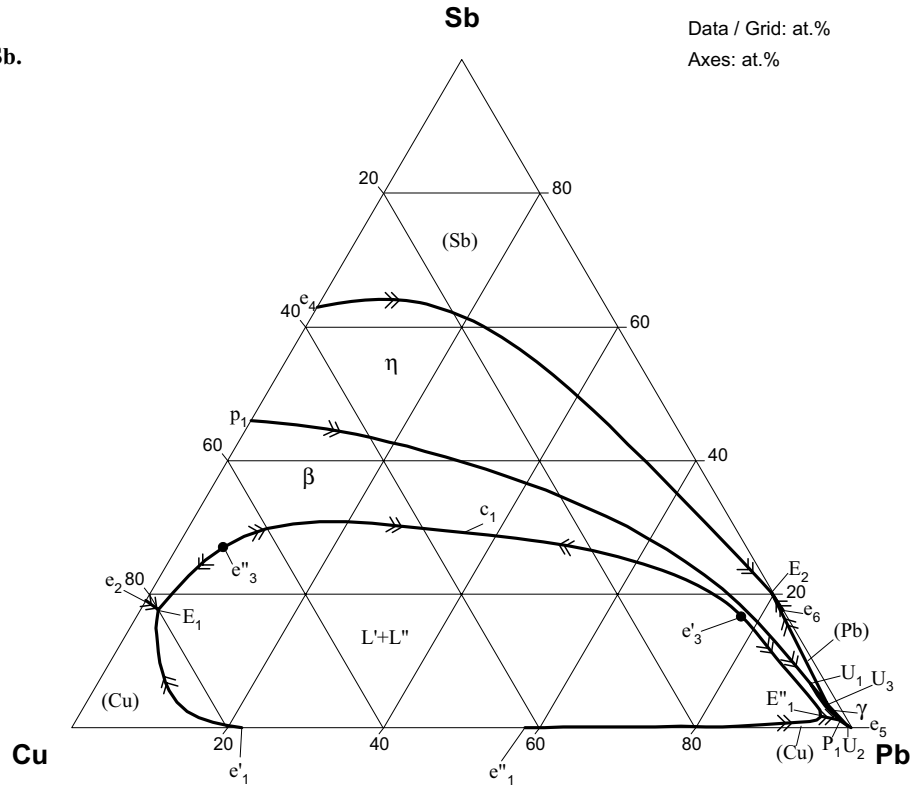

Fig. 2a: Cu-Pb-Sb.
Liquidus surface

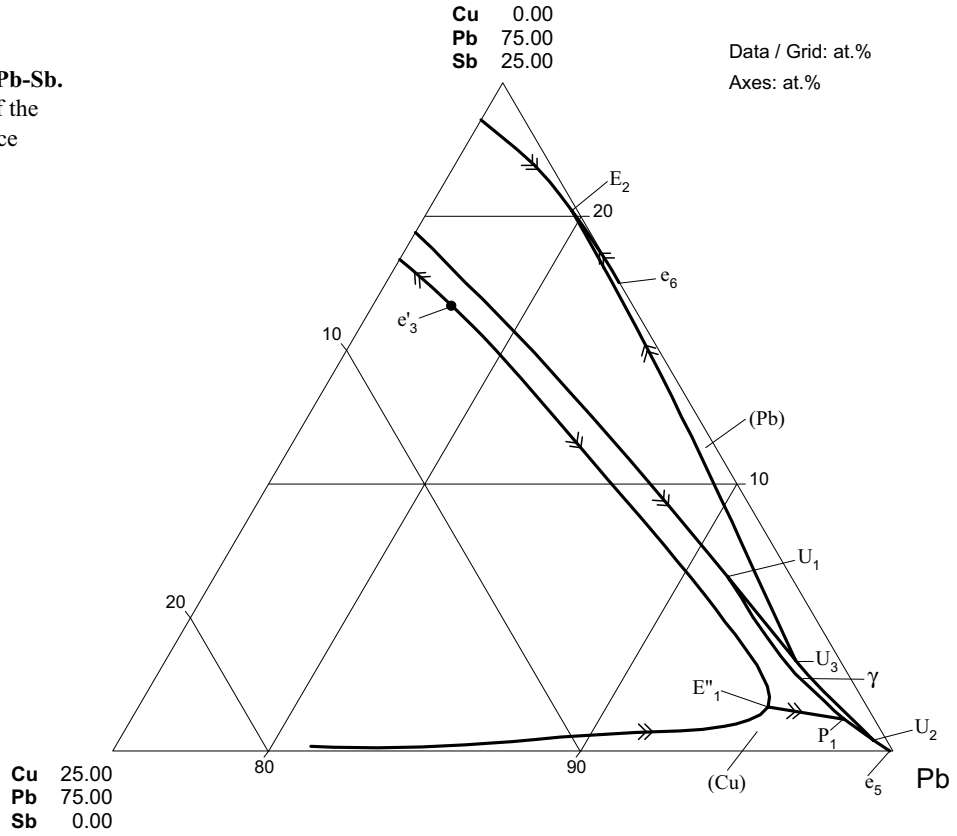

Fig. 2b: Cu-Pb-Sb.
Pb rich part of the liquidus surface (enlargement)

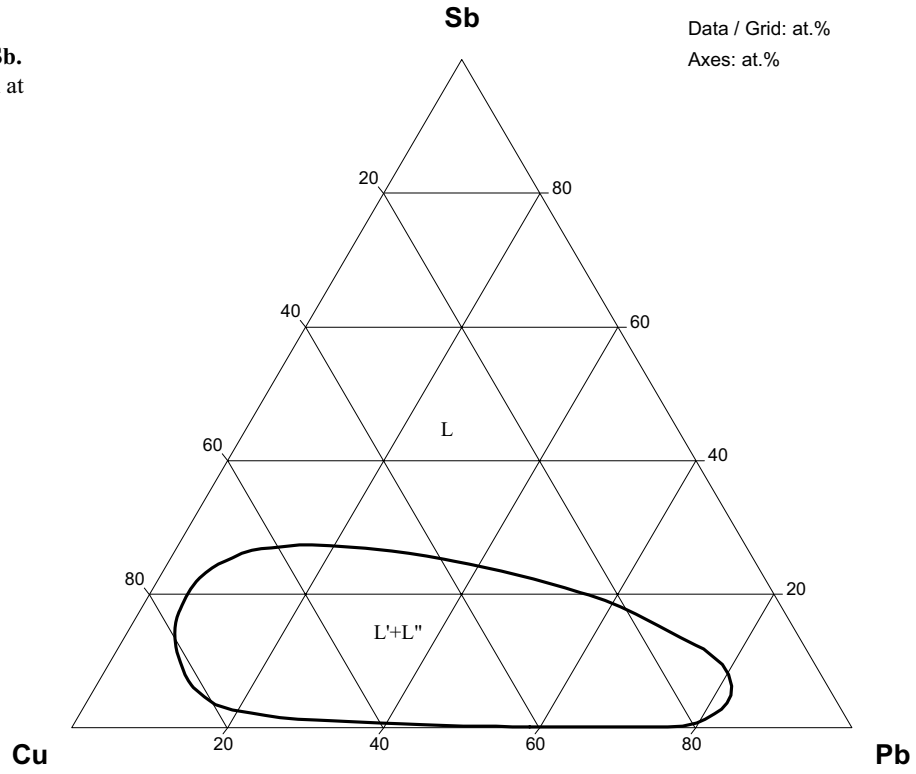

Fig. 3: Cu-Pb-Sb. Isothermal section at 1200°C

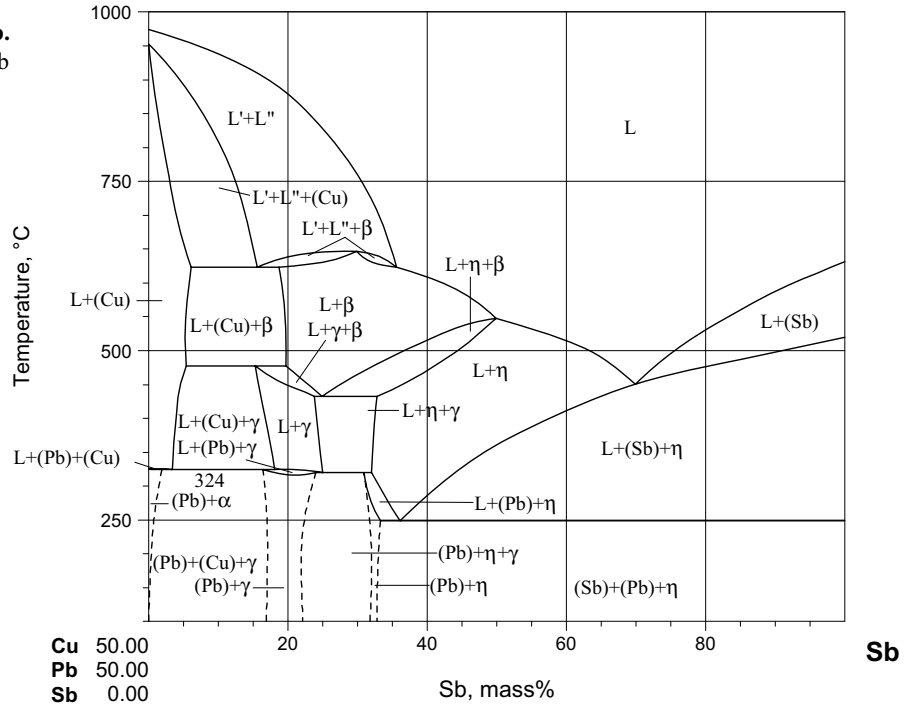

Fig. 4: Cu-Pb-Sb. The $Cu_{76.5}Pb_{23.5}$-Sb vertical section

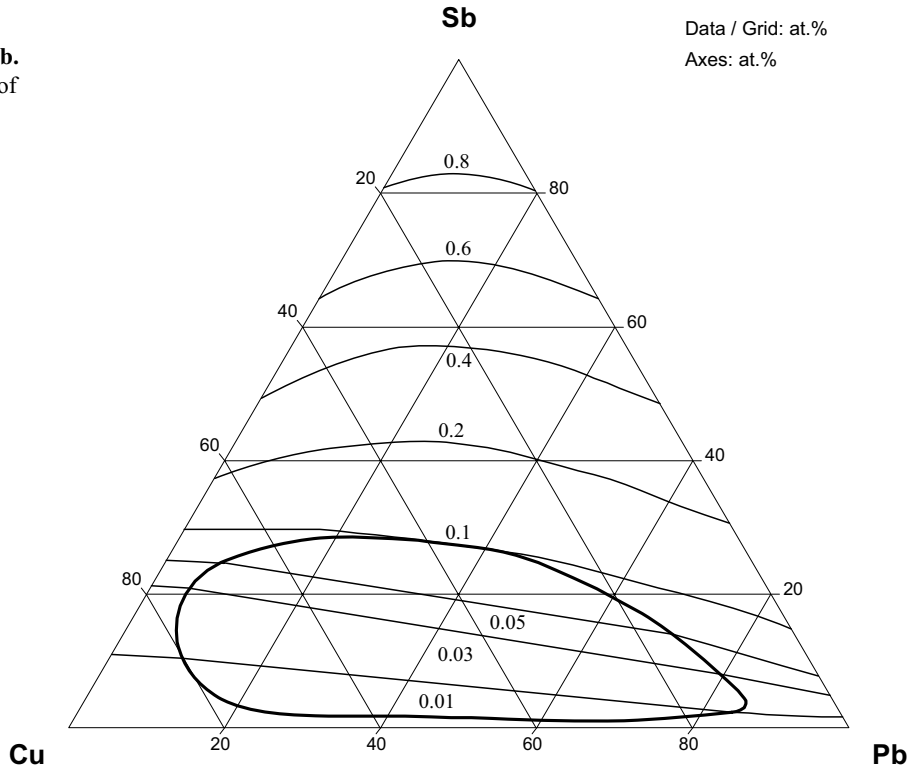

Fig. 5: Cu-Pb-Sb. Isoactivity curves of Sb at 1200°C

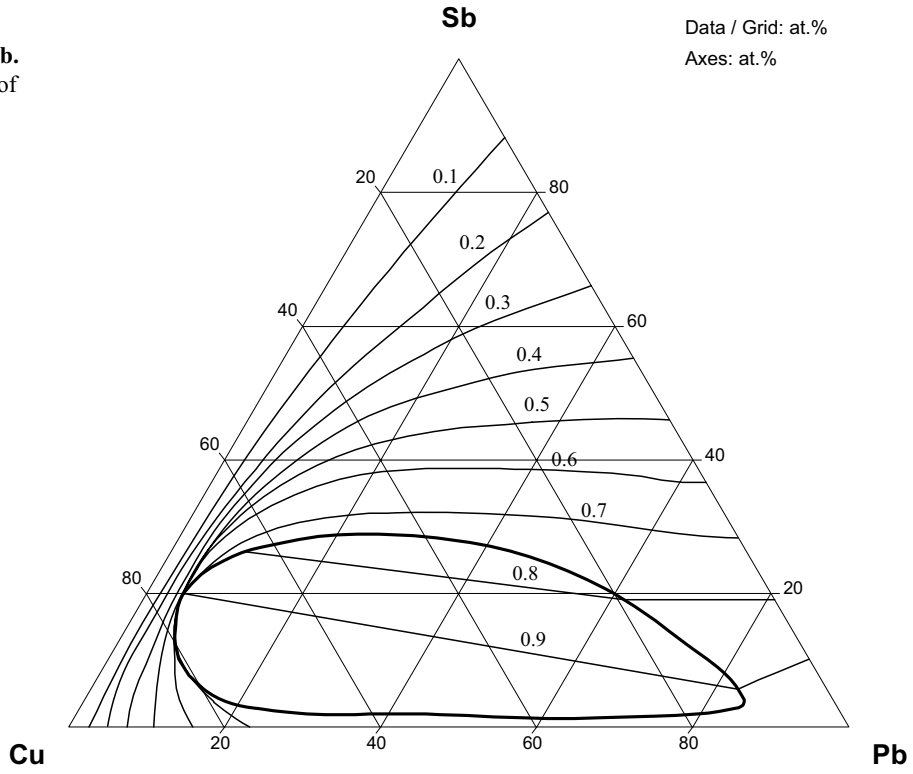

Fig. 6: Cu-Pb-Sb. Isoactivity curves of Pb at 1200°C

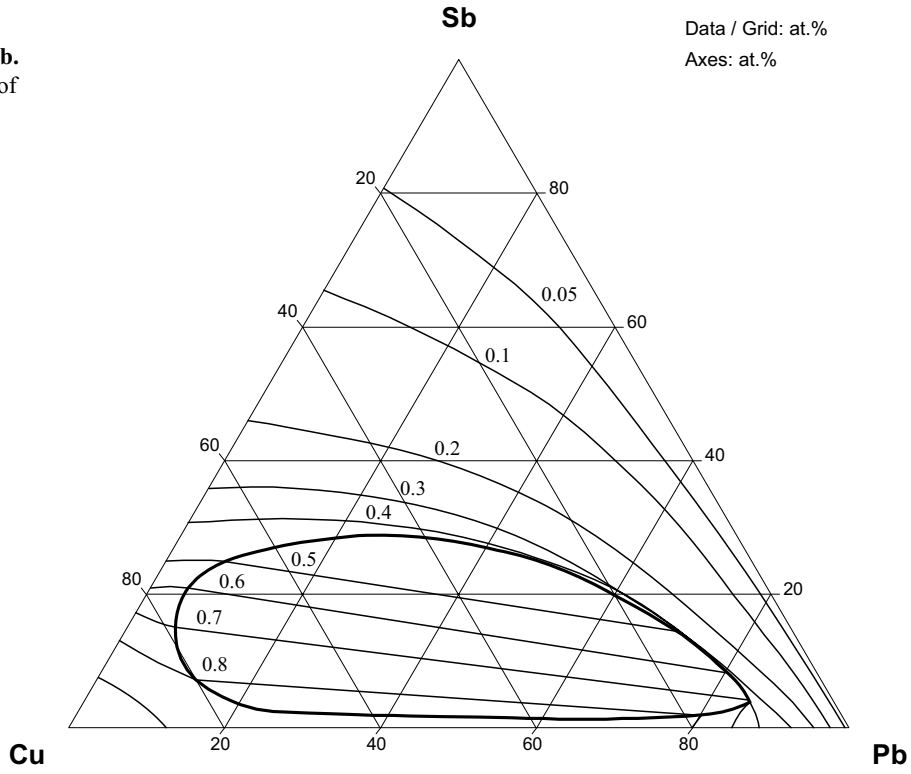

Fig. 7: Cu-Pb-Sb. Isoactivity curves of Cu at 1200°C